

Differential photoelectron distributions in a strong elliptically polarized low-frequency laser field

S. P. Goreslavskii and S. V. Popruzhenko

Moscow State Engineering and Physics Institute, 115409 Moscow, Russia

(Submitted 10 April 1996)

Zh. Éksp. Teor. Fiz. **110**, 1200–1215 (October 1996)

We investigate the polarization dependences of momentum, angular, and energy distributions and ionization rates for field and atomic parameters corresponding to the regime of optical tunneling. We describe the evolution of the differential distributions as the polarization changes from circular to linear. In particular, we show that over a wide range of ellipticities the angular distribution is extended along the small axis of the polarization ellipse in the direction transverse to the maximum electric field. Only for very small ellipticities does the distribution readjust to extend along the electric field, i.e., the case of a linearly polarized field. For the momentum and angular distributions we obtain closed analytic expressions valid for arbitrary ellipticity. © 1996 American Institute of Physics. [S1063-7761(96)00510-0]

1. INTRODUCTION

In recent years there has been a continuing expansion of the frontiers of experimental and theoretical investigations of the nonlinear ionization of atoms and molecules in the optical tunneling regime, for which the Keldysh adiabaticity parameter is less than unity. Under these conditions, the simple Amosov–Delone–Krainov ionization probability, which is based on the idea of tunneling, is commonly used to describe the measured ion output.^{1,2} For the next generation of experiments, in which both the ionization mechanism itself and accompanying processes that generate high harmonics will be investigated, a more detailed description is required, which includes the energy and angular distributions, as well as their dependence on the laser polarization. Interest in the dependence on polarization has increased in connection with discussions of harmonic generation in an elliptically polarized field.³

Simple analytic expressions that describe the momentum distribution of photoelectrons in the tunneling regime are known for the special cases of circular and linear polarization (expressions and citations can be found in Refs. 1 and 4). In a circularly polarized field, the angular distribution possesses axial symmetry relative to the direction of propagation of the field, and the spectrum has a maximum near an energy equal to the average vibrational energy. In a field with linear polarization, the angular distribution is axially symmetric relative to the direction of the polarization, and the maximum in the energy spectrum occurs at low energies.

The goal of this paper is to trace the transition as the ellipticity changes between these significantly different expressions for the distributions, and as far as possible to describe this evolution using analytic expressions that reveal the basic dependence on the field and atomic parameters. This goal can be achieved in principle by taking the tunneling limit of the more general expressions based on the Keldysh–Faisal–Reiss (KFR) approach (reviewed in Ref. 5) and used for arbitrary values of the adiabaticity parameter. For an elliptically polarized field, the angular distributions in the form of a sum over above-threshold peaks are known for

short-range potentials⁶ and for a zero-range potential.^{7,8} In this case, however, it is found that the expressions in the tunneling regime given in Ref. 6 give the correct limiting transition to linear polarization, but do not describe the transition to circular polarization. Meanwhile, in Refs. 7 and 8 the probability amplitude for an individual above-threshold peak is expressed in terms of an infinite sum of products of two Bessel functions (generalized Bessel functions according to Ref. 5). Expressions of this type are ill-suited for computations in the tunneling regime, where a large number of partial contributions have comparable values.

In this work, our starting point for calculating the differential distributions of electrons during ionization by an elliptically polarized field in the tunneling regime will be the ordinary starting expressions of the KFR model in the vector potential gauge.⁵ The main difference between our approach and that of previous workers is that in our case the contribution to the transition amplitude from a single optical period is calculated without using a Fourier expansion.^{9,10} The consequences of this approach are twofold. First of all, the picture of a strong low-frequency field inducing a quantum ionization transition that is not smeared out over multiple harmonics turns out, as it does in a circular field,⁹ to be analogous to that of Landau–Zener transitions between time-dependent electron terms. Secondly, the calculations can be considerably simplified, in particular by avoiding the appearance of generalized Bessel functions and obtaining a closed expression in terms of elementary functions for the momentum distribution of the photoelectrons for arbitrary values of the ellipticity. A preliminary qualitative analysis of this distribution reveals the nontrivial character of the evolution of the angular distribution between the circular and linear polarizations.¹¹

In the next section we discuss our formulation of the problem; in Sec. 3 we derive the momentum distribution of photoelectrons. Then integration yields the angular distribution (Sec. 4), the energy spectrum (Sec. 5), and the ionization rate (Sec. 6). The last section consists of summarizing comments.

2. STARTING EQUATIONS

A laser field with constant amplitude F , frequency ω , and ellipticity ξ is specified by the vector potential

$$\mathbf{A}(t) = (cF/\omega)(\cos(\omega t), \xi \sin(\omega t), 0), \quad (1)$$

which corresponds to an electric field

$$\mathbf{F}(t) = F(\sin(\omega t), -\xi \cos(\omega t), 0). \quad (2)$$

According to the KFR model, the ionization is treated as a quantum transition from a bound state ψ_i with ionization potential I to a state of the continuum, which is approximated by the nonrelativistic solution of Volkov $\psi_p(t)$. The ionization rate is defined by the relation

$$dW(\mathbf{p}) = 2\pi |B(\mathbf{p})|^2 \sum_n \delta\left(\frac{\mathbf{p}^2}{2} + I + U - n\omega\right) \frac{d^3p}{(2\pi)^3} \quad (3)$$

with a transition amplitude per period equal to

$$B(\mathbf{p}) = \psi_i(\mathbf{p}) \left(\frac{\mathbf{p}^2}{2} + I\right) \frac{\omega}{2\pi} \int_0^{2\pi/\omega} dt \times \exp\left\{i \int_0^t dt_1 [I + \varepsilon_p(t_1)]\right\}. \quad (4)$$

Here $\varepsilon_p(t) = m\mathbf{v}^2(t)/2$ and $\mathbf{v}(t) = \mathbf{p} + \mathbf{A}(t)/c$ are respectively the time-dependent kinetic energy and velocity of a classical electron with canonical momentum \mathbf{p} in the field (1), while $U = (1 + \xi^2)F^2/4\omega^2$ is the average vibrational energy in this field; $\psi_i(\mathbf{p})$ is the wave function of the initial state in the momentum representation. Atomic units $e = \hbar = m = 1$ are used, and the electron charge equals -1 .

In short optical pulses, where the acceleration due to the transverse gradient force is negligible, the canonical momentum is a constant of the motion, so that an electron is detected outside the field with momentum \mathbf{p} and energy $\mathbf{p}^2/2$ (provided the energy satisfies one of the conservation laws in (3)).

In the optical tunneling regime, the characteristic energies of the problem satisfy the condition

$$\omega < I < U. \quad (5)$$

The left-hand inequality implies that the field is low-frequency, while the right-hand is equivalent to the assertion that the field is strong and the Keldysh parameter is less than unity: $\gamma = \omega\sqrt{2I}/F < 1$. We will also assume

$$F < F_a = (2I)^{3/2}, \quad (6)$$

i.e., the field is weaker than the atomic field.

3. MOMENTUM DISTRIBUTION

An integration of (3) over energy, taking into account the δ -functions, would convert it into a sum of angular distributions belonging to individual above-threshold peaks. In the tunneling regime the terms of this sum depend smoothly on the index of the above-threshold peak, and the sum over n can be replaced by an integral. With this fact in mind, let us immediately replace the sum in (3) by an integral and carry out the integration over the continuous variable n with the help of the δ -functions. This allows us to obtain the momen-

tum distribution of photoelectrons (the ionization rate within an element of momentum space d^3p) in the form

$$dW(\mathbf{p}) = 2\pi |B(\mathbf{p})|^2 d^3p / (2\pi)^3 \omega. \quad (7)$$

The dependence on the energy $\varepsilon = \mathbf{p}^2/2$ in (7) corresponds to the envelope of the above-threshold peaks, while the ratio $d\varepsilon/\omega$ gives the number of above-threshold peaks in the integration energy interval $d\varepsilon$.

The next step is to calculate the amplitude $B(\mathbf{p})$. Under tunneling-regime conditions (5) the exponential in the integral (4) oscillates rapidly. For a large portion of an optical period, the instantaneous frequency $\varepsilon_p(t) + I$ of the oscillation is a quantity of order $U > I, \omega$. The oscillations are slowed in the vicinity of the point (or points) t_0 where the kinetic energy is a minimum, i.e., $\dot{\varepsilon}_p(t_0) = 0$. Neighborhoods of these points give the main contribution to the integral. Near such a minimum we expand $\varepsilon_p(t)$ in a series, retaining contributions quadratic in $t - t_0$, and carry out the trivial integration in the exponential. After extending the limits of integration to $\pm\infty$, the outer integral in (4) can be expressed in terms of an Airy function, which by virtue of condition (6) can be replaced by its asymptotic representation for large values of the argument. Replacement of the Airy function by its asymptotic form is equivalent to using the method of steepest descent in the time integral. The momentum distribution finally takes the form

$$dW(\mathbf{p}) = \omega \{IF^2(t_0)[I + \varepsilon_p(t_0)]\}^{1/2} \times \exp\left\{-\frac{\sqrt{2}}{3} \frac{[I + \varepsilon_p(t_0)]^{3/2}}{F(t_0)}\right\} \frac{d^3p}{(2\pi)^3}. \quad (8)$$

In addition to the transformations mentioned above, we have substituted in (8) the explicit form of the wave function for a potential of zero radius, $|\psi_i(\mathbf{p})(p^2/2 + I)|^2 = \sqrt{2I}$, and have replaced the second derivative according to the equation $\ddot{\varepsilon}_p(t_0) = F^2(t_0)$. An explanation of these replacements will be given below.

Since we now know the value of the second derivative, we can estimate the width $(t - t_0)_{tr}$ of the effective region in the integral (4). This time is naturally interpreted as the time for a quantum transition to the continuum. It is determined by the condition that the quadratic term in the expansion of the kinetic energy $F^2(t_0)(t - t_0)_{tr}^2/2$ becomes the same order of magnitude as the ionization potential. The time for a transition is found to be exactly equal to the tunneling time $(t - t_0)_{tr} = \sqrt{2I}/F$ through the potential barrier introduced by Keldysh,¹² and the quantity $\gamma = \omega(t - t_0)_{tr}$ coincides with the adiabaticity parameter. In the tunneling regime, the transition time constitutes a small fraction of the optical period.

When the laser field is weaker than the atomic field, the properties of the distribution (8) are determined primarily by the exponential. Finding the maximum of the distribution reduces to investigating the extrema of the exponential. From its structure, however, it is quite obvious that the maximum of the distribution occurs at those momenta \mathbf{p} for which at the time of the transition $t_0 = t_0(\mathbf{p})$ the kinetic energy equals zero and the field is a maximum. Thus, the semiclassical model of Corkum¹³ can be extended to a field with arbitrary elliptical polarization.

If the kinetic energy $\varepsilon_{\mathbf{p}}(t)$ has two minima separated in time during one period, as will take place for polarizations close to linear, then the transition amplitude takes the form

$$B(\mathbf{p}) = B_0(\mathbf{p}) + B_1(\mathbf{p}) \exp(S_{01}), \quad (9)$$

where S_{01} is the phase difference of the function under the integral sign at the stationary points. Under conditions (5) this difference is large, and the contributions of the two points do not interfere, so that the probability equals the sum of the probabilities calculated at each of the points using (8).

In the exposition that follows, it is convenient to introduce the field momentum into the discussion:

$$\mathbf{p}_F(t) = \frac{1}{c} \mathbf{A}(t).$$

In the course of an optical period the vector $\mathbf{p}_F(t)$ describes an ellipse in momentum space that lies in the plane of polarization of the laser field. We will refer to this as the field ellipse (do not confuse this with the ellipse described by the electric field vector (2)). The kinetic energy takes the form

$$\varepsilon_{\mathbf{p}}(t) = \frac{1}{2} [\mathbf{p}_{\perp} + \mathbf{p}_F(t)]^2 + \frac{1}{2} p_z^2. \quad (10)$$

An absolute minimum of the kinetic energy equal to zero is achieved only when the momentum \mathbf{p} lies on the field ellipse. In this case we have $p_z = 0$, and the transverse component of the velocity reduces to zero at the instant of time when the field ellipse is antiparallel to \mathbf{p} , i.e.,

$$\mathbf{v}_{\perp}(t_0) = \mathbf{p} + \mathbf{p}_F(t_0) = 0. \quad (11)$$

From this we find the relation between the phase of the field ωt_0 and ϕ for vectors \mathbf{p} lying in the field ellipse, where ϕ is the azimuthal angle of the vector:

$$\cot(\omega t_0) = \xi \cot \phi, \quad (12)$$

and also the field at the transition time:

$$F(t_0(\mathbf{p})) = F \sqrt{1 - (1 - \xi^2) p_x^2 / p_F^2}. \quad (13)$$

For momenta \mathbf{p} that do not lie on the field ellipse, the kinetic energy at the transition time $\varepsilon_{\mathbf{p}}(t_0)$ is nonzero, which in fields below the atomic value leads to a sharp decrease in the distribution (8). Thus, the momentum distribution is concentrated in a thin tube around the field ellipse. In general, the distribution along the tube axis is nonuniform due to the momentum dependence of the field at the transition time. The small transverse size of the effective region allows us to simplify Eq. (8) considerably. First of all, for momenta that do not lie on the field ellipse but are sufficiently close to it we can use Eqs. (12) and (13). By direct calculation it is easy to verify that if $\mathbf{v}_{\perp}(t_0) = 0$ holds, then we have $\ddot{\varepsilon}_{\mathbf{p}}(t_0) = F^2(t_0)$, which we already used in (8). Secondly, we can expand the exponential in small deviations around its minimum value, and neglect the quantity $\varepsilon_{\mathbf{p}}(t_0)$ in the preexponential factor along with the ionization potential. It still remains to obtain the explicit dependence of $\varepsilon_{\mathbf{p}}(t_0)$ on momentum. For this, we begin by using the equation

$$\begin{aligned} \dot{\varepsilon}_{\mathbf{p}}(t_0) = \sin(\omega t_0) [p_x + p_F \cos(\omega t_0)] \\ - \xi \cos(\omega t_0) [p_y + \xi p_F \sin(\omega t_0)] = 0, \end{aligned} \quad (14)$$

which determines the position of the kinetic energy minimum. We then eliminate from (9) the term that contains the momentum projection p_x ; then, taking (12) into account, we eliminate the field phase ωt_0 . We find

$$\varepsilon(\mathbf{p}, \xi) = \frac{1}{2} \lambda(\phi) \{ p_{\perp} \sqrt{\sin^2 \phi + \xi^2 \cos^2 \phi} - \xi p_F \}^2 + \frac{1}{2} p_z^2, \quad (15)$$

where

$$\lambda(\phi) = \frac{\sin^2 \phi + \xi^4 \cos^2 \phi}{\sin^2 \phi + \xi^2 \cos^2 \phi}. \quad (16)$$

Here and in what follows, we will use the notations $p_{\perp} = p \sin \theta$, $p_z = p \cos \theta$, and $p_x = p \sin \theta \cos \phi$. The angle θ is measured from the z axis, while the azimuthal angle ϕ is measured from the large axis of the polarization ellipse. An immediate result of these transformations is the first term in the momentum distribution:

$$\begin{aligned} \frac{dW}{d^3p} = A \exp \left[\frac{F_a}{6IF} \gamma^2 (1 - \xi^2) p_x^2 \right] \left\{ \exp \left[- \frac{F_a}{FI} \varepsilon(\mathbf{p}, \xi) \right] \right. \\ \left. + \exp \left[- \frac{F_a}{FI} \varepsilon(\mathbf{p}, -\xi) \right] \right\}, \\ A = \frac{1}{4\pi^2} \frac{\omega}{F} \exp \left(- \frac{2F_a}{3F} \right). \end{aligned} \quad (17)$$

The second term in (17) comes from taking into account the second minimum according to (9) as a function of $\varepsilon_{\mathbf{p}}(t)$. In a linearly polarized field ($\xi = 0$), two symmetric minima occur when $p_x + p_F \cos(\omega t_0) = 0$ (it is assumed that $|p_x| < p_F$). As the ellipticity increases from zero, the symmetry of the minima is destroyed; one of them becomes the principal minimum (i.e., the value of $\varepsilon_{\mathbf{p}}(t)$ is smaller there), while the second (additional) minimum is lifted upward and rapidly disappears, after which there is only one minimum per period. For a given momentum $\mathbf{p} = (p_x, p_y, p_z)$, at the time where the additional minimum occurs the kinetic energy of an electron with momentum $(p_x, -p_y, p_z)$ has a value that coincides with the principal minimum (and conversely). In the kinetic energy (10), a change in sign of p_y is equivalent to a change in the sign of ξ ; this is also taken into account in writing the second term in (17).

The momentum distribution (17) possesses symmetries that are natural in the presence of an elliptically polarized field: it is unchanged by reflecting the momentum vector relative to the axes of the polarization ellipse and relative to the plane of the polarization.

The effective region of the distribution (17) consists of a thin tube around a certain portion of the field ellipse that depends on ξ . The transverse width of the tube in momentum-space, $\sqrt{2FI/F_a}$, is small compared to an atomic momentum and does not depend on the ellipticity. In a circularly polarized field the effective region contains the entire

circle of radius p_F . For $\xi < \xi_4 = 1 - F/F_a$ the only vectors contained in the effective region are those with

$$|p_x| \leq (p_x)_{\text{eff}} = p_F [F/F_a (1 - \xi^2)]^{1/2}.$$

i.e., the portions of the field ellipse around the ends of the large axis are eliminated. As ξ decreases, the width $(p_x)_{\text{eff}}$ decreases. The transverse components of the momenta in the effective regions are quantities of order $(p_y)_{\text{eff}} = \xi p_F$. For an ellipticity $\xi_3 = \sqrt{F/F_a}$ the widths $(p_x)_{\text{eff}}$ and $(p_y)_{\text{eff}}$ are the same $((p_y)_{\text{eff}} > (p_x)_{\text{eff}}$ for $\xi > \xi_3$). Finally, for an ellipticity $\xi_1 = \gamma \sqrt{F/F_a}$ the small axis of the field ellipse becomes comparable to the radius of the tube, i.e., the effective region is converted into a cylinder of length $p_F \sqrt{F/F_a}$.

In the region $\xi \ll 1$ the distribution (17) can be simplified. Expanding (15) and (16) in powers of ξ everywhere except for the narrow intervals of azimuthal angles $|\phi| \leq \xi \ll 1$ and $|\pi - \phi| \leq \xi \ll 1$, we find $\lambda = 1$ and

$$p_{\perp} \sqrt{\sin^2 \phi + \xi^2 \cos^2 \phi} = p_{\perp} |\sin \phi|.$$

As will be clear in what follows, the range of ϕ that is important to the distribution is much wider than the intervals we have discarded. The leading term of the expansion equals

$$\begin{aligned} \frac{dW}{d^3p} = & A \exp\left(-\frac{F_a}{6IF} \gamma^2 p_x^2\right) \exp\left(-\frac{F_a}{2IF} p_z^2\right) \\ & \times \left\{ \exp\left[-\frac{F_a}{2IF} (|p_y| - \xi p_F)^2\right] \right. \\ & \left. + \exp\left[-\frac{F_a}{2IF} (|p_y| + \xi p_F)^2\right] \right\}. \end{aligned} \quad (18)$$

The discarded contributions in the exponential are small compared with unity for $\xi \leq \gamma$ and $\xi \leq \sqrt{F/F_a}$. These bounds are the conditions of applicability of Eq. (18). The restored ellipticity enters into (18) in the form of the ratio ξ/ξ_1 , which in this region of applicability can be both larger and smaller than unity. Since Eq. (18) is symmetric, we can omit the absolute value notation.

If we set $\xi = 0$ in (17) and (18), we obtain the momentum distribution in a linearly polarized field:^{1,4}

$$\frac{dW}{d^3p} = 2A \exp\left[-\frac{F_a}{2IF} \left(p_z^2 + p_y^2 + \frac{\gamma^2 p_x^2}{3}\right)\right], \quad (19)$$

which possesses axial symmetry relative to the direction of polarization; its maximum is at the point $\mathbf{p} = 0$.

In the limit $\xi \rightarrow 0$ the terms in curly brackets in (18) and (17) are equal to one another, which corresponds to symmetric minima for $\varepsilon_p(t)$ in a linearly polarized field. When the ellipticity is not too small, i.e., for $\xi > \xi_1$, the first term reaches its maximum value of unity on the field ellipse, while the second remains exponentially small for any momenta. Strictly speaking, the second term should always be absent when ξ exceeds that ξ_c for which the second minimum $\varepsilon_p(t)$ disappears. In order to avoid complicating the form of the expressions, we prefer to use (17) for all values of the ellipticity, since the exponentially small correction that we retain makes practically no difference in the momentum distribution.

The momentum distribution for small ellipticity can be obtained by another method that differs from the one given above. Solving Eq. (14) by iteration on the small parameter ξ and substituting

$$\cos(\omega t_{0,1}) = -\frac{p_x}{p_F}, \quad \sin(\omega t_{0,1}) = \mp \sqrt{1 - \left(\frac{p_x}{p_F}\right)^2}$$

into (8), (9) as a zeroth-order approximation, after expanding in $(p_x/p_F)^2 \ll 1$ we once more are led to (18).

The photoelectron momentum distribution in an elliptically polarized field is obtained from Ref. 6 if we double the overall coefficient in (17), and use Eq. (18) for the sum in curly brackets, in which we must discard the second term and delete the absolute value on p_y in the first term. Without the absolute value sign, the distribution becomes asymmetric with respect to the interchange $p_y \rightarrow -p_y$.

For $\xi = 1$ Eq. (17) becomes the well-known expression for a circularly polarized field:^{1,4,10}

$$\frac{dW}{d^3p} = A \exp\left\{-\frac{F_a}{2IF} [p_z^2 + (p_{\perp} - p_F)^2]\right\}. \quad (20)$$

This distribution is axially symmetric with respect to the direction of propagation of the field. Its maximum occurs at a momentum $p_{\perp} = p_F$, $p_z = 0$, at which the electron energy equals the average vibrational energy $F^2/2\omega^2$. The effective region consists of a circular torus of radius p_F with a transverse tube width $\sqrt{2FI/F_a}$ that is small not only compared to p_F but also compared to the atomic momentum.

A simplified form of the expression that describes the approach of the momentum distribution to the form (20) is obtained by expanding (17) in the parameter $(1 - \xi^2)\cos^2 \phi \ll 1$. This parameter is small in two cases: first, when the polarization is close to circular, i.e., due to the factor $1 - \xi^2$; the angle ϕ in this case can be arbitrary, and secondly, for azimuthal angles ϕ around $\pi/2$, where the cosine is small. As is clear from (17), it is at these angles where the maximum occurs in the ϕ -dependence, as long as the factor $1 - \xi^2$ is of order unity, i.e., the polarization is not too close to circular. The region of applicability of this approximation is determined by the condition $\xi_3 \leq \xi \leq 1$ and encompasses a rather wide range of ellipticities. In all of this region the exponentially small terms in (17) can be discarded. We finally obtain

$$\begin{aligned} \frac{dW}{d^3p} = & A \exp\left[-\frac{F_a}{6IF} \gamma^2 (1 - \xi^2) p_{\perp}^2 \cos^2 \phi\right] \\ & \times \exp\left\{-\frac{F_a}{2IF} [(p_{\perp} - p_{\perp}(\phi))^2 + p_z^2]\right\}, \end{aligned} \quad (21)$$

where

$$p_{\perp}(\phi) = \varepsilon p_F [1 + (1/2)(1 - \xi^2)\cos^2 \phi]. \quad (22)$$

It is clear from (21) and (22) that as long as $1 - \xi < \gamma \sqrt{F/F_a}$ holds the distribution remains close to (20); in this case, the field ellipse differs from a circle $p_{\perp} = p_F$ by less than the width of the distribution over the entire perimeter. As ξ departs further from unity the position of the maximum of the distribution with respect to the variable p_{\perp} depends on ϕ , which begins to affect the dependence of the

first exponential in (21) on azimuthal angle. This latter effect remains weak provided that $\xi_4 < \xi \leq 1$ holds. Further increasing the deviation $1 - \xi$ until the ellipticity lies in the interval $\xi_3 \ll \xi < \xi_4$ introduces a large factor $\xi^2 F_a / F = \xi^2 / \xi_3^2 \gg 1$ in the exponential, and a maximum in the distribution with respect to azimuthal angle around $\pi/2$. The width of the maximum is a quantity of order

$$(\pi/2 - \phi)_{\text{eff}} = [\xi^2(1 - \xi^2)F_a/F]^{-1/2} \ll 1. \quad (23)$$

The dependence of the momentum distribution on azimuthal angle is radically simplified if we neglect the small second term in (22), which gives

$$\frac{dW}{d^3p} = A \exp\left[-\frac{F_a}{6IF} \gamma^2(1 - \xi^2)p_{\perp}^2 \cos^2 \phi\right] \times \exp\left[-\frac{F_a}{2IF} [(p_{\perp} - \xi p_F)^2 + p_z^2]\right]. \quad (24)$$

For ξ in the interval $\xi_3 \ll \xi < \xi_4$ this simplification of the exponential is possible when $\sqrt{F/F_a} < \gamma\xi$. In order for the interval of ellipticities that satisfy this requirement to be truly significant, the strong inequality $\sqrt{F/F_a} \ll \gamma$ must hold, which is equivalent to $\gamma \gg (\omega/2I)^{1/3}$ or $F/F_a \ll (\omega/2I)^{2/3}$, i.e., the field cannot be too strong. Let us recall that the value of the field is bounded from below by the assumption $\gamma < 1$. Transforming the last factor in (24) to the form

$$\exp\left[-\frac{F_a}{2IF} [(p - \xi p_F)^2 + 2\xi p_F p(1 - \sin \theta)]\right]$$

shows that due to the large factor F_a/IF in the distribution we can set $p = \xi p_F$ everywhere except where the deviation $p - \xi p_F$ is very small. Similar considerations allow us to expand $1 - \sin \theta$ in a series, and in other places set $\sin \theta = 1$. As a result we obtain a distribution that is factored in the spherical variables:

$$\frac{dW}{d^3p} = A \exp\left[-\frac{F_a}{2IF} (p - \xi p_F)^2\right] \exp\left[-\frac{F_a}{IF} \xi^2 p_F^2 \left(\frac{\pi}{2} - \theta\right)^2\right] \exp\left[-\frac{F_a}{3F} \xi^2(1 - \xi^2) \cos^2 \phi\right]. \quad (25)$$

In the next sections we discuss the angular distribution, the energy spectrum, and the total ionization rate calculated by integrating the distribution (17) and its approximate forms.

4. ANGULAR DISTRIBUTION

The quadratic dependence of the exponential on the magnitude of the momentum in (17) allows us to carry out the integration over this variable analytically and obtain an angular distribution in the form¹¹

$$\frac{dW(\theta, \phi)}{d\Omega} = D \frac{h}{g^{3/2}} \exp\left[-\left(\frac{\xi}{\xi_1}\right)^2 f\right]. \quad (26)$$

Here D is a constant, while f, g , and h are functions of the spherical angles defined as follows:

$$D = \frac{\omega}{4\pi^2} \sqrt{\frac{F}{F_a}} \exp\left(-\frac{2F_a}{3F}\right),$$

$$g(\theta, \phi) = \cos^2 \theta + \sin^2 \theta \sin^2 \phi + \left[\frac{1}{3} \gamma^2(1 - \xi^2) + \xi^4\right] \sin^2 \theta \cos^2 \phi,$$

$$f(\theta, \phi) = \frac{\lambda(\phi)}{g(\theta, \phi)} \left[\cos^2 \theta + \frac{1}{3} \gamma^2(1 - \xi^2) \sin^2 \theta \cos^2 \phi \right],$$

$$h(\theta, \phi) = \frac{\sqrt{\pi}}{g(\theta, \phi)} \left[\frac{1}{2} + \left(\frac{\xi}{\xi_1}\right)^2 \lambda(\phi) (\sin^2 \phi + \xi^4 \cos^2 \phi) \sin^2 \phi \right].$$

After a preliminary qualitative analysis and discussion of limiting cases, we turn to the results of direct tabulation based on Eq. (26). As a function of the angle θ the distribution is concentrated near the polarization plane, i.e., near $\theta = \pi/2$. In Fig. 1, we give a series of curves listed in order of decreasing ellipticity that clearly portray the complicated evolution of the angular distribution in the plane of polarization as the ellipticity changes. In accordance with the character of these curves, we can identify four stages.

1) The distribution is isotropic in ϕ for $\xi = 1$ (the corresponding horizontal line is not shown on the figure) and is close to isotropic in the narrow interval of ellipticities $\xi_4 < \xi \leq 1$ (curves 1 in Fig. 1a).

2) The distribution is extended along the small axis of the polarization ellipse, i.e., photoelectrons are emitted primarily in the direction perpendicular to the field maximum (curves 2 and 3 in Fig. 1a). The maximum around $\phi = \pi/2$ forms rapidly for small changes in ξ in the neighborhood of ξ_4 and is retained over a wide interval of ellipticities $\xi_3 < \xi < \xi_4$.

3) There is a transition region for $\xi_2 = \gamma(F/F_a)^{1/3} < \xi < \xi_3$. Decreasing ξ in the vicinity of ξ_3 qualitatively changes the form of the angular distribution: around $\phi = 0$ (and also around $\phi = \pi$), i.e., in the direction of the major axis of the polarization ellipse, a second maximum appears that is at first weaker but which grows rapidly. At the same time the height of the first maximum decreases, and its position shifts from $\pi/2$ towards $\phi = 0$ (curves 4–7 in Fig. 1b,c). The trace of the first maximum disappears completely for $\xi = \xi_2$. Curve 8 shows a situation close to this (Fig. 1c). The value of ξ_2 is found by investigating the derivative of (26).

4) For $\xi < \xi_2$ the distribution with a single maximum is extended along the large axis of a strongly oblate polarization ellipse (curve 9 in Fig. 1c). However, it strongly resembles the distribution in a linearly polarized field only for very small $\xi < \xi_1 = \gamma\sqrt{F/F_a}$.

Over a wide range of ellipticities $\xi_3 < \xi \leq 1$ the exponential in (26) contains a large factor $(\xi/\xi_1)^2 = (\xi/\xi_3 \gamma)^2$, and so for $\theta = \pi/2$, $\phi = \pi/2$ even a quite small deviation of the nonnegative function f from zero leads to a rapid decrease in the distribution. Expanding in $(1 - \xi^2) \cos^2 \phi \ll 1$, retaining the

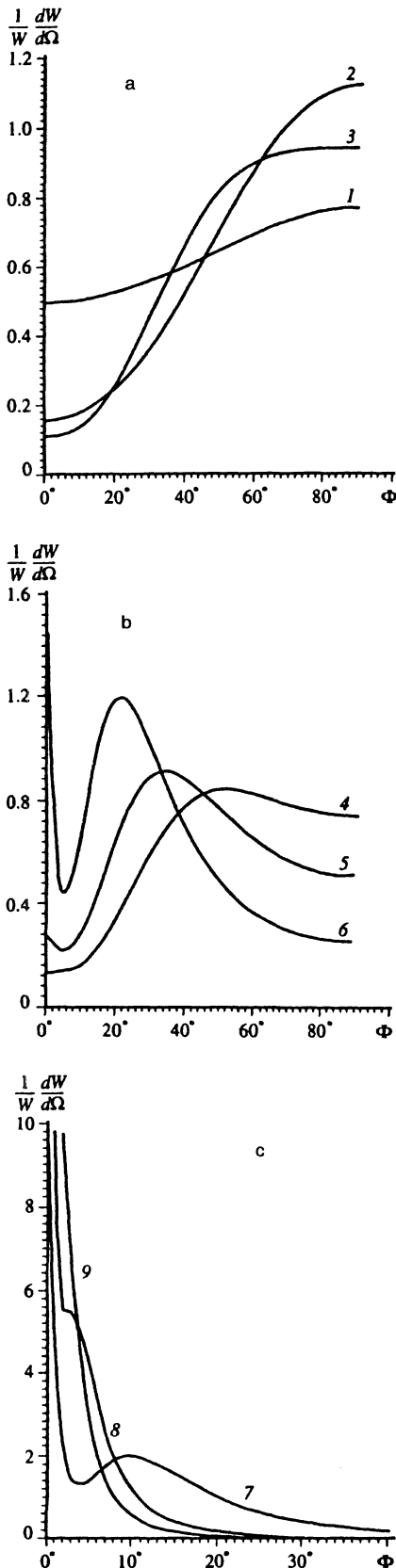


FIG. 1. Distribution with respect to azimuthal angle in the plane of polarization $\theta = \pi/2$ calculated using (26). In view of the symmetry only the first quadrant is shown. The distribution is normalized to unit area. The values of the parameters were as follows: $\omega = 0.1$ eV, $I = 13.6$ eV, $F = 2.9 \cdot 10^8$ V/cm. In this case we have $\gamma = 0.074$, $F/F_a = 0.056$, $\xi_1 = 0.017$, $\xi_2 = 0.028$, $\xi_3 = 0.22$, $\xi_4 = 0.95$. The curves are labeled in order of decreasing ellipticity: 1— $\xi = 0.95$, 2—0.70, 3—0.50, 4—0.40, 5—0.30, 6—0.20, 7—0.10, 8—0.030, 9—0.015.

first term, and taking into account that the angle θ is close to $\pi/2$, we find $\lambda = 1$, $g = 1$, $h = \sqrt{\pi}(\xi/\xi_1)^2$, and the angular distribution takes the form

$$\frac{dW}{d\Omega} = \sqrt{\pi} D \left(\frac{\xi}{\xi_1} \right)^2 \exp \left\{ - \left(\frac{\xi}{\xi_1} \right)^2 \left[\cos^2 \theta + \frac{1}{3} \gamma^2 (1 - \xi^2) \sin^2 \theta \cos^2 \phi \right] \right\}. \quad (27)$$

It is clear from (27) that the effective deviation from the plane of polarization equals $(\pi/2 - \theta)_{\text{eff}} = \gamma \xi_3 / \xi$. It increases with decreasing ellipticity, but in the interval $\xi_3 < \xi \leq 1$ it remains small compared to unity.

For $\xi = 1$ there is no dependence on the azimuthal angle in (27). For $\xi \neq 1$ the distribution has a maximum at $\phi = \pi/2$ and a minimum at $\phi = 0$. As long as the difference between ξ and unity is small enough that $1 - \xi^2$ cancels the large factor $(\xi/\xi_1)^2$, the distribution is smooth and does not differ much from isotropic, i.e., its values at the maximum and minimum are comparable in magnitude (curve 1 in Fig. 1a). Near an ellipticity $\xi_4 = 1 - F/F_a$ there is a reconstruction of the distribution, due to the fact that for $\xi < \xi_4$ the coefficient in front of $\cos^2 \phi$ in (21) becomes large: a maximum forms in the direction of the small axis of the polarization ellipse (curves 2 and 3 in Fig. 1a). The width of this maximum is given by Eq. (23). It decreases as ξ decreases until $\xi^2 = 1/2$. As the ellipticity decreases further towards $\xi^2 < 1/2$, the width begins to increase, approaching a value of order unity as ξ approaches $\xi_3 \ll 1$ (curve 4 in Fig. 1b). This considerable increase in width, which in fact makes the distribution isotropic in azimuthal angle in the neighborhood of ξ_3 , is an intermediate stage in the process of converting a distribution which is extended along the small axis of the polarization ellipse into a distribution extended along its large axis, which is appropriate for a linearly polarized field.

A limiting form of (27) can be obtained by integrating the momentum distribution (24) directly. Note that in order for (26) to become (27) it is enough to ensure $\xi_3 < \xi \leq 1$, whereas (24) was obtained under more rigorous assumptions.

Although characteristic values of the ellipticity are small compared with unity in the transition region, Eq. (25) cannot be significantly simplified. As long as $\xi_1 \leq \xi$ holds, the angular distribution forms as a result of the combined influences of three factors: the functions h , g , and the exponentials. Only for very small ellipticities $\xi < \xi_1$ is the distribution determined by the single factor $g^{-3/2}$, and thus coincides with the distribution in a linearly polarized field up to corrections of order $(\xi/\xi_1)^2 \ll 1$:

$$\frac{dW}{d\Omega} = \sqrt{\pi} D \left[2 \left(\sin^2 \alpha + \frac{1}{3} \gamma^2 \cos^2 \alpha \right)^{3/2} \right]^{-1}. \quad (28)$$

In (28) the function g is written in terms of the spherical angles α, β , which are natural for the case of linear polarization along the x axis (here, α is the angle with the x axis and β is the angle of rotation around the x axis). These angles are related to the angles θ, ϕ by the expressions $\sin \theta \cos \phi = \cos \alpha$, $\sin \theta \sin \phi = \sin \alpha \cos \beta$ and $\cos \theta = \sin \alpha \sin \beta$. For this way of writing the expressions the axial symmetry of the angular distribution around the direction of polarization be-

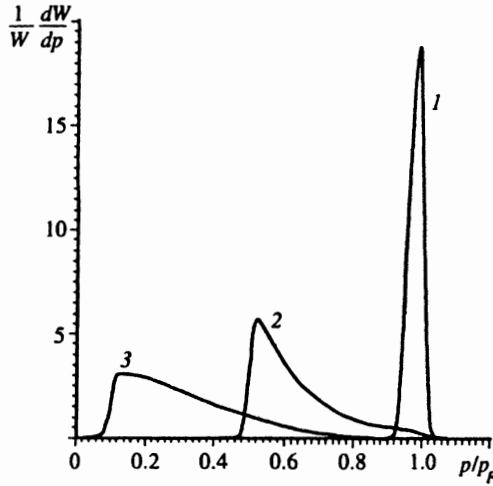


FIG. 2. Distribution of photoelectrons with respect to the magnitude of the momentum obtained by numerical integration of (17). Normalization to unit area. The values of the field parameters are the same as in Fig. 1. The curves are given for three values of ξ : 1—0.95, 2—0.50, 3—0.10.

comes obvious. Since $\gamma < 1$ holds, the angular distribution has sharp maxima at $\alpha = 0$ and at $\alpha = \pi$, around which we can limit ourselves to the first term in a Taylor series for the expressions in curly brackets of (28). By retaining the trigonometric functions we can describe both maxima in a unified way. However, if the expansion is used, the area under each maximum equals half the total probability.

5. ENERGY SPECTRUM

In contrast to the angular distribution, we were unable to obtain a single expression for the energy spectrum that can be used for arbitrary ellipticities. Figure 2 shows the results of a numerical integration of the momentum distribution (17) over angles. Actually, we are now discussing the distribution with respect to the magnitude $p = \sqrt{2\varepsilon}$ of the momentum. The plots shown illustrate the general features of the evolution of the spectrum as the ellipticity varies from one to zero. At first the narrow maximum in the distribution shifts with decreasing ξ in toward lower energies, preserving its width almost unchanged as it does so. Starting with a certain value of the ellipticity, the peak becomes asymmetric because the width increases from the high-energy side, but the maximum continues its motion towards low energies.

Fairly simple analytic expressions for the spectrum are obtained in the limiting cases of large and small values of ξ . Integrating the factorized distribution (25), we find

$$\frac{dW}{dp} = \xi \sqrt{\frac{IF}{2\pi F_a}} \exp(-z) I_0(z) \exp\left(-\frac{2F_a}{3F}\right) \times \exp\left[-\frac{F_a}{2IF}(p - \xi p_F)^2\right], \quad (29)$$

where $z = (F_a/6IF)\xi^2(1 - \xi^2)$ and

$$I_0(z) = \frac{1}{\pi} \int_0^\pi d\theta \exp(\mp z \cos \theta)$$

is a modified Bessel function. The product $\exp(-z)I_0(z)$ is a monotonic function with simple asymptotic forms:

$$\exp(-z)I_0(z) = \begin{cases} 1, & z \ll 1, \\ 1/\sqrt{2\pi z}, & z \gg 1. \end{cases} \quad (30)$$

For $\xi = 1$ we obtain from (29) and (30) the well-known spectrum in a circularly polarized field.^{1,4} When the deviation from circular polarization is large enough, we have

$$\frac{dW}{dp} = \frac{IF}{\pi F_a} \sqrt{\frac{3}{2(1 - \xi^2)}} \exp\left(-\frac{2F_a}{3F}\right) \times \exp\left[-\frac{F_a}{2IF}(p - \xi p_F)^2\right]. \quad (31)$$

The position of the maximum and the width of the spectrum determined by Eq. (29) agree over a wide interval $\xi_3 < \xi \leq 1$ with the results of numerical integration of the momentum distribution (17), although the approximate form (25) has a narrower range of applicability.

For small ellipticities, the spectrum is obtained by integrating (18). Taking into account both terms in curly brackets of (18), we have

$$\frac{dW}{dp} = 4\pi D p^2 \exp\left[-\frac{1}{3}\left(\frac{p}{p_1}\right)^2\right] R\left(\frac{p}{p_0}, \frac{\xi}{\xi_1}\right), \quad (32)$$

where the function of two variables $R(p, \xi)$ is defined as

$$R(p, \xi) = 2 \int_0^1 dt \frac{t}{\sqrt{1-t^2}} I_0(2\xi p t) \exp(-p^2 t^2 - \xi^2). \quad (33)$$

The distribution (32) has two considerably different scales, $p_0 = \sqrt{2FI/F_a}$ and $p_1 = p_F \sqrt{F/F_a}$, whose ratio $p_0/p_1 = \gamma \ll 1$.

Let us first consider the case of linear polarization $\xi = 0$. Since $R(0,0) = 2$, as $p \rightarrow 0$ the spectrum reduces to zero due to the statistical weight p^2 . As p increases, starting in the vicinity of the smaller scale p_0 the function R decreases as p^{-2} and the product $p^2 R(p/p_0, 0)$ remains constant. After this point, the spectrum is determined by the exponential factor with the large scale p_1 . In short, the energy spectrum has a markedly asymmetric maximum at a low energy $\varepsilon_0 = p_0^2/2 = IF/F_a$. It falls to zero over a narrow interval $0 < \varepsilon < \varepsilon_0$ and decreases exponentially, but over the large scale $\varepsilon_1 = p_1^2/2 = (F/F_a)p_F^2/2$ it falls off in the direction of higher energies. If the narrow dip is ignored, then we can say that the spectrum has a maximum at $\varepsilon = 0$. The width of the spectrum is determined by the large scale, i.e., $\varepsilon_1 \propto F^3$. This form of the spectrum is preserved as long as $\xi < \xi_1$.

For $\xi > \xi_1$ the behavior of R (and accordingly the spectrum) is the same as for $\xi = 0$ when $p > (\xi/\xi_1)p_0 = \xi p_F$. For $p < \xi p_F$ the function R is proportional to $\exp[-(p - \xi p_F)^2/p_0^2]$. This property is easily derived by replacing the function I_0 in the integral (33) by its asymptotic form for large arguments according to (30). In addition to the statistical weight, yet another factor appears to suppress the spectrum in the region of small p . The dip around the coordinate origin widens and extends out to an energy $(\xi p_F)^2/2 > \varepsilon_0$, which now marks the maximum in the spectrum. The existence of a maximum at these energies and its

asymmetric shape were noted in Ref. 14. This situation is preserved as long as $\xi < \xi_3$ holds. Thus, it turns out that for all except the very smallest ξ the position of the maximum in the energy spectrum is still determined by the same ratio $p_{\max} = \xi p_F$.

6. TOTAL PROBABILITY

Integrating (29) gives the ionization rate for $\xi > \xi_3$ in the form

$$W = I \frac{\xi F}{F_a} \exp\left(-\frac{2F_a}{3F}\right) \exp(-z) I_0(z). \quad (34)$$

Taking into account the asymptotic form (30), for $\xi=1$ we obtain the well-known result for circular polarization:

$$W_{\text{cir}} = I \frac{F}{F_a} \exp\left(-\frac{2F_a}{3F}\right), \quad (35)$$

while for a sufficiently large deviation of ξ from unity, i.e., in the interval $\xi_3 < \xi < \xi_4$, Eq. (34) becomes

$$W = I \sqrt{\frac{3}{\pi(1-\xi^2)}} \left(\frac{F}{F_a}\right)^{3/2} \exp\left(-\frac{2F_a}{3F}\right). \quad (36)$$

The ionization rate for small ξ is found by integrating the momentum distribution (18). These results coincide with (36), although the regions of applicability of the functions (29) and (18) under the integral sign do not even overlap.

In discussing the reason for this agreement, it is convenient to deal with the dimensionless transition probability per optical period, $w_1 = 2\pi W/\omega$. Neglecting numerical coefficients, this can be written in the form

$$w_1 \propto \frac{F_a}{F} \exp\left(-\frac{2F_a}{3F}\right) \frac{\Gamma(\xi)}{F_a}. \quad (37)$$

The first factor here is the transition probability per period to a quantum state corresponding to the maximum of the distribution (17). This probability naturally does not depend on the field frequency, since the transition takes place within a small fraction of the period. The second factor is the number of quantum states in the phase volume where the transition can occur efficiently. According to the discussion of Sec. 2, this volume equals the product of the cross-sectional area of the effective tube and the effective length of arc of the field ellipse:

$$\Gamma(\xi) = (2IF/F_a) L_{\text{eff}}. \quad (38)$$

For all ξ except those very close to unity we have $L_{\text{eff}} = (p_x)_{\text{eff}}$, where

$$(p_x)_{\text{eff}} = p_F \sqrt{\frac{F}{F_a}} \frac{1}{\sqrt{1-\xi^2}}, \quad (39)$$

So (35)–(37) are equivalent to Eq. (34). The agreement of the expressions for the total probability for different ξ is not an accident, but rather is related to the fact that $(p_x)_{\text{eff}}$ is determined by the same Eq. (39) over the entire interval $0 < \xi < \xi_4$. For ξ close to unity we have $L_{\text{eff}} = 2\pi p_F$, and (37) and (38) are equivalent to (35).

An ionization rate closely resembling (34) and (36) in structure was obtained via the adiabatic approach of Ref. 15.

7. CONCLUSION

The photoelectron distributions given in this paper apply to ionization of an s -state in a potential with zero radius. Introduction of a factor $C_{\kappa 0}^2$ (see Ref. 15) into the corresponding expressions extends these results to the case of a short-range potential.

In the strong-field approximation (SFA) it is assumed⁵ that if we use an atomic wave function as the initial state, the transition amplitude (4) describes ionization in a Coulomb field. Recently it was shown¹⁶ that inclusion of the Coulomb correction to the phase of the final (Volkov) state in fact converts a matrix element involving the wave function of the hydrogen atom ground state into a matrix element for the potential of zero radius (up to a factor). Then our distributions and probabilities describe ionization from the ground state of hydrogen after multiplying by $2(2F_a/F)^2$ (see Ref. 16).

Our derivation of the momentum distribution shows that the assertion of the semiclassical model¹³ that the ionization takes place at a time when the field is a maximum and the instantaneous kinetic energy of an electron equals zero also holds for an elliptically polarized field. It is this need to simultaneously satisfy both conditions that leads to an angular distribution extended along the major axis of the polarization ellipse in the direction perpendicular to the maximum field for intermediate values of the ellipticity.

In the physical picture that follows from our calculations (see also (9)), in which ionization by a strong low-frequency field is viewed as a Landau–Zener transition, increasing the field amplitude does not lead to qualitative changes such as conversion of the tunneling regime to an above-barrier regime. Like the numerical calculations of Refs. 17 and 18, the changes in the probability and distributions are quantitative in character. As the field intensity approaches atomic levels, the overall tendency is one of significant increase in the width of the distribution. In particular, at $\xi^2 = 1/2$ the width of the distribution with respect to azimuthal angle is $(\pi/2 - \phi)_{\text{eff}} = 30^\circ$ even for $F/F_a = 0.1$.

Note that our expressions give the dependence on ξ for fixed values of the field F , and thus for varying light intensities. In order to obtain expressions that apply to a fixed intensity $I_* = (c/4\pi)F_*^2$, it is necessary to replace F everywhere by $F_*(1+\xi^2)^{-1/2}$. This replacement does not significantly change the results, since the additional factor that depends on ellipticity is of order unity.

A region of considerable interest is the narrow interval of ellipticities in which the angular and energy distributions retain the form characteristic of a linearly polarized field. This interval is bounded from above by the product of two small parameters of the theory: $\xi < \gamma\sqrt{F/F_a}$. For values $I = 1.36$ eV, $\omega = 0.1$ eV, $\gamma = 0.074$, $F/F_a = 0.05$ this condition gives $\xi < 1.5\%$.

An experimental investigation of this dramatic evolution of the differential photoelectron distribution as the polarization changes from circular to linear could be a critical test of

the postulated mechanism for ionization by a strong low-frequency field. In contrast to the differential distribution, the total ionization rate varies smoothly with ellipticity over a wide range; the comparatively abrupt change takes place only near circular polarization.

The authors are grateful to N. B. Delone and V. P. Kraĭnov, and also to the participants in N. B. Delone's seminar at the General Physics Institute, Russian Academy of Sciences, for stimulating discussions.

This work was carried out with the support of the Russian Fund for Fundamental Research (Grant No. 95-02-06056-1A). One of the authors (S. V. Popruzhenko) is grateful to the International Science Foundation for a student grant.

- ¹N. B. Delone and V. P. Kraĭnov, *Multiphoton Processes in Atoms*, p. 70. Springer-Verlag, Berlin, 1994.
²F. A. Ilkov, J. E. Decker, and S. L. Chin, *J. Phys. B: At. Mol. Opt. Phys.* **25**, 4005 (1992).
³N. B. Delone and V. P. Kraĭnov, *J. Opt. Soc. Amer. B* **8**, 1207 (1992).
⁴P. Dietrich, N. H. Burnett, M. Ivanov, and P. B. Corkum, *Phys. Rev. A* **50**, R3585 (1994).
⁵H. R. Reiss, *Prog. Quant. Electron.* **16**, 1 (1992).

- ⁶A. M. Perelomov, V. S. Popov, and M. V. Terent'ev, *Zh. Éksp. Teor. Fiz.* **51**, 309 (1966) [*Sov. Phys. JETP* **24**, 207 (1967)].
⁷M. Bashkansky, P. H. Bucksbaum, and D. W. Schumacher, *Phys. Rev. Lett.* **59**, 274 (1987).
⁸W. Becker, A. Lohr, and M. Kleber, *Quantum Semiclass. Opt.* **7**, 423 (1995).
⁹S. P. Goreslavskii, *Zh. Éksp. Teor. Fiz.* **108**, 456 (1995) [*JETP* **81**, 245 (1995)].
¹⁰H. R. Reiss and V. P. Kraĭnov, in *Proc. 15th Int. Conf. on Coherent and Nonlinear Optics Technical Digest: Superintense Laser Fields*, St. Petersburg, Russia, 1995.
¹¹S. P. Goreslavskii and S. V. Popruzhenko, *Laser Phys.* **6**(4) (1996).
¹²L. V. Keldysh, *Zh. Éksp. Teor. Fiz.* **47**, 1945 (1964) [*Sov. Phys. JETP* **20**, 1307 (1964)].
¹³P. B. Corkum, N. H. Burnett, and F. Brunel, *Phys. Rev. Lett.* **62**, 1259 (1989).
¹⁴R. V. Karapetyan, in *Abstracts of the Intl. Conf. on Multiphoton Processes (ICOMP V)*, Paris, France, 1990, p. 195.
¹⁵A. M. Perelomov, V. S. Popov, and M. Terent'ev, *Zh. Éksp. Teor. Fiz.* **50**, 1393 (1966) [*Sov. Phys. JETP* **23**, 924 (1966)].
¹⁶V. P. Kraĭnov and B. Shorki, *Zh. Éksp. Teor. Fiz.* **107**, 1180 (1995) [*Sov. Phys. JETP* **80**, 657 (1995)].
¹⁷K. C. Kulander, *Phys. Rev. A* **36**, 2726 (1987).
¹⁸R. Shakeshaft, R. M. Potvliege, M. Dorr *et al.*, *Phys. Rev. A* **42**, 1656 (1990).

Translated by Frank J. Crowne